



# Measuring Apoptosis and Necrosis Cell Populations by Heat and Compound Induction using the Cellometer Vision

WHITE PAPER



Nexcelom Bioscience LLC. | 360 Merrimack Street, Building 9 | Lawrence, MA 01843  
T: 978.327.5340 | F: 978.327.5341 | E: [info@nexcelom.com](mailto:info@nexcelom.com) | [www.nexcelom.com](http://www.nexcelom.com)

1001248 Rev. A

# Measuring Apoptosis and Necrosis Cell Populations by Heat and Compound Induction using the Cellometer Vision

## Introduction

Recently, a new imaging cytometry system has been developed by Nexcelom Bioscience LLC (Lawrence, MA, USA) for fluorescence-based cell population analysis [1, 2]. Originally, the system has been used for automated cell concentration and viability measurement using disposable counting slides with both bright-field (BR) and fluorescent (FL) imaging methods [3]. The system has recently been demonstrated to perform fast and accurate cell population analysis comparable to the traditional flow cytometry method. Cellometer image cytometry systems can perform fluorescence-based cell death assays, which can provide a quick, simple, and inexpensive alternative method for smaller biomedical research laboratories.

In this study, we demonstrate the use of Cellometer imaging cytometry for rapid necrosis/apoptosis detection. In order to show the capability of the system, heat-induced and drug-induced cell death assays are performed. Necrosis is purposely induced in Jurkat cells by incubating at high temperatures. For drug-induced cell death, alpha-tocopherylsuccinate ( $\alpha$ -TOS), a vitamin E analogue that has been shown to induce apoptosis through the intrinsic pathway (mitochondrial destabilization) was used [4, 5]. In addition, cytotoxicity dose-response comparison was measured for both  $\alpha$ -TOS and 2-amino-N-quinoline-8-yl benzenesulfonamide (QBS) [6]. QBS can induce apoptosis by arresting cell cycle, while  $\alpha$ -TOS induces by inhibiting proliferation of cells, and both compounds have been known for its anti-cancer effects. The Cellometer imaging cytometry was used to measure FITC labeled Annexin V and propidium iodide (PI) fluorescence to identify and quantify the apoptotic and necrotic cell populations, respectively. The experimental results were evaluated to validate the imaging cytometric capabilities of the Cellometer system as compared to the conventional flow cytometry.

## Materials and Methods

### *Cell preparation*

The Jurkat cell line (TIB-152) was cultured in RPMI 1640 medium. The cell culture was maintained in an incubator at 37°C with 5% CO<sub>2</sub>.

### *Heat-induced necrosis*

The Jurkat cell culture was separated into five flasks that were incubated in water baths heated to 37, 45, 50, 55, and 60°C. The cells were then fluorescently stained using commercially available kits for flow and imaging cytometric analysis.

### *Drug-induced apoptosis*

$\alpha$ -TOS was used to induce apoptosis in the Jurkat cells [4, 5, 7] and the results were compared to those obtained by flow cytometry. The compound was dissolved in DMSO.

After first validating the detection method, additional dose-response experiments were performed using  $\alpha$ -TOS and QBS. The Jurkat cells were prepared using the same protocol described above. Next, they were incubated in 14 flasks containing  $\alpha$ -TOS (100, 80, 60, 40, 30, 20, and 10  $\mu$ M), QBS (100, 10, 1, 0.1, 0.01, and 0.001  $\mu$ M), and a control with media only. The Jurkat cells were allowed to incubate for 96 h and were then fluorescently stained.

### *Staining procedure*

Annexin V Binding Buffer and Annexin V-FITC (fluorescein isothiocyanate) was used for apoptotic cell staining, and propidium Iodide (PI) was used for necrotic cell staining. After both heat and drug-treated incubation periods, the Jurkat cells were resuspended in Annexin V Binding Buffer. Annexin V-FITC and PI were added and each stained sample was incubated before performing flow and imaging cytometric analysis.

### *Flow cytometry analysis*

Fluorescence intensity data of heat and drug-induced Jurkat cells were acquired from a FACSCalibur flow cytometer (BD Biosciences, San Jose, CA, USA). A “Blue” (488 nm) excitation laser was used for both FITC and PI emission channels. The measured results were analyzed using the De Novo Software and compared with results from Cellometer imaging cytometry.

### *Cellometer imaging cytometry analysis*

The Cellometer instrumentation has been described previously, here [1].

Two filter sets, VB-535-402 and VB-660-502, were used in Cellometer Vision for Annexin V-FITC and PI detection, respectively. A fluorescent threshold in the software was set to 0% in order to measure total fluorescence of each counted cell from the captured images. The measured fluorescence intensities and counts were exported to Excel for analysis in the De Novo Software. The results were compared to the flow cytometry data.

## Results

*Figure 1. Heat-induced necrosis images.*

- (1a) Apoptotic Jurkat cells emitted bright green fluorescence and necrotic cells emitted strong red fluorescence. As the temperature increased, the number of green apoptotic and red necrotic cells also increased.
- (1b) The fluorescence intensity scatter plot at each incubation temperature for flow cytometry and Cellometer. The bottom left of the quadrant represents the viable cells (Annexin V negative, PI negative), the bottom right represents the apoptotic cells (Annexin V positive, PI negative), the upper right represents the necrotic cells (Annexin V positive, PI positive), and the upper left represents debris (nonspecific fluorescence). Heat treatment resulted in a dose-dependent increase of necrotic cells in the population. As the temperature increased from 37 to 60°C, the necrotic cell population increased dramatically from 2.4 to 86.8% and 7.0 to 81.6%, for flow cytometry and Cellometer Vision, respectively.
- For the apoptotic cell population, there was a mild increase initially that was followed by a fall to the basal level due to the fact that apoptotic cells had become necrotic at higher temperatures. Clear separations of viable, apoptotic, and necrotic cells were observed in both Cellometer and flow cytometry data. Other than the 55°C sample, the results obtained from Cellometer and flow cytometry were highly similar.

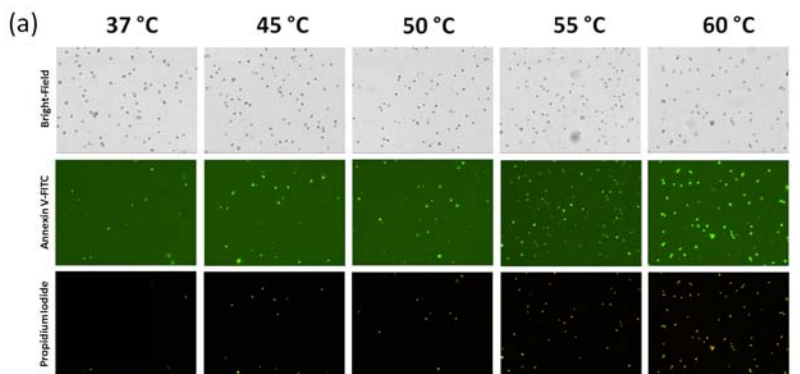
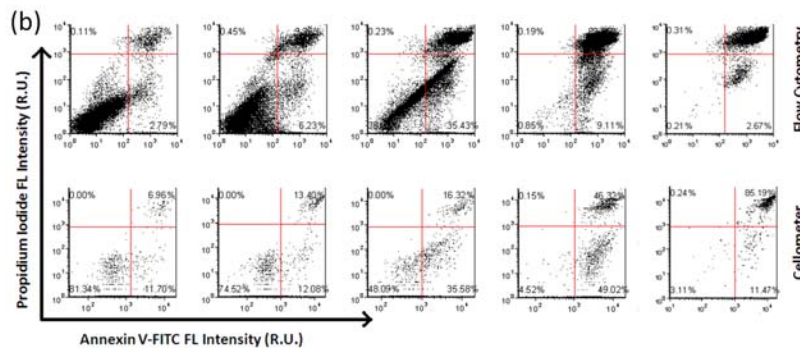


**Figure 1.** Heat-induced necrosis in Jurkat cells. a) Bright-field (top row) and fluorescent images of Annexin V-FITC (middle row) and PI (bottom row) at each incubation temperature. b) Fluorescent intensities were plotted using Annexin V-FITC with respect to PI for flow cytometry (top row) and Cellometer (bottom row).



**Figures 2 and 3. Drug-induced apoptosis.**

- (2a and 3a) Fluorescent images of drug-induced Jurkat cells captured by Cellometer. In both incubation times, the apoptotic and necrotic Jurkat cells were clearly identified by the green and red fluorescence, which were used to generate the fluorescence intensity scatter plot of Annexin V-FITC with respect to PI. Similar trends were observed for both incubation times. Visually, the number of apoptotic cells (green) increased as the concentration of  $\alpha$ -TOS increased. In contrast, the number of red necrotic cells remained relatively constant for across the concentrations.
- (2b and 3b) The fluorescence intensity scatter plots at each  $\alpha$ -TOS concentration for flow cytometry and Cellometer are shown for 24 and 48 h incubation, respectively. As  $\alpha$ -TOS increased, no significant difference was observed for the necrotic cell population, which held true for both incubation times. For apoptotic cells, the population increased from 1.2 to 24.8% and 4.0 to 25.8%, at 24 h incubation for flow cytometry and Cellometer, respectively. For 48 h incubation, the apoptotic cell population increased from 1.2 to 27.7% and 4.0 to 29.5%, for flow cytometry and Cellometer, respectively. The apoptosis results corresponded closely ( $\pm 5\%$ ) between Cellometer and flow cytometry at all tested concentrations and incubation times.

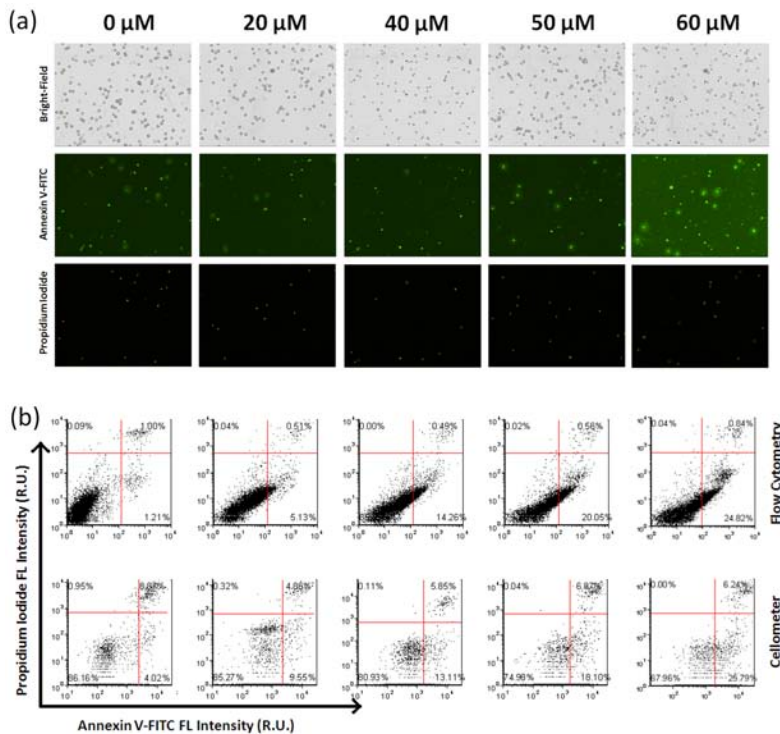


**Figure 2.** Drug-induced apoptosis in Jurkat cells at 24 h incubation time. a) Bright-field (top row) and fluorescent images of Annexin V-FITC (middle row) and PI (bottom row) at each incubation concentration. b) Fluorescent intensities were plotted using Annexin V-FITC with respect to PI for flow cytometry (top row) and Cellometer (bottom row).

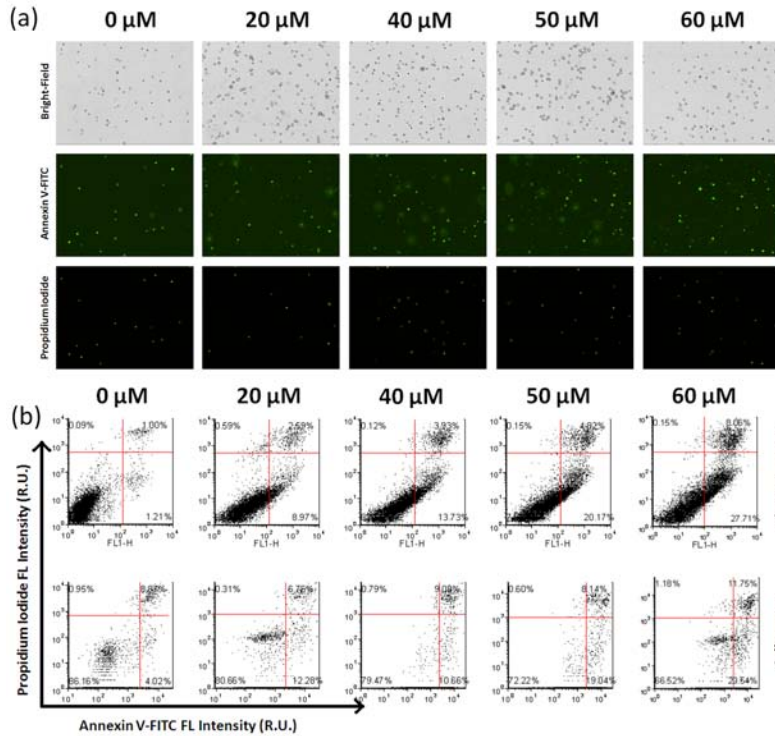


**Figure 3.** Drug-induced apoptosis in Jurkat cells at 48 h incubation time. a) Bright-field (top row) and fluorescent images of Annexin V-FITC (middle row) and PI (bottom row) at each incubation concentration. b) Fluorescent intensities were plotted using Annexin V-FITC with respect to PI for flow cytometry (top row) and Cellometer (bottom row).

**Figure 4. Cytotoxicity dose–response analysis.**

- (4a) The viability dose–response curves for heat-induced samples are shown. There was a clear negative correlation between the temperature and viability of Jurkat cells. Similar trends were observed in both the Cellometer and flow cytometry data. Although the PI positive and Annexin V positive percentages did not correlate for the 55°C sample, the quantitative viability difference between these two groups of measurements was less than 15%.
- (4b and c) The viability dose–response curves for drug-induced samples are shown for 24 and 48 h incubation respectively. For 24 h incubation, the viability dropped from 86.2 to 70.3% for Cellometer and 97.7 to 74.3% for flow cytometry. For 48 h incubation, the viability dropped from 86.2 to 67.6% for Cellometer, and 97.7 to 64.1% for flow cytometry. The differences between these two groups ranged from 5 to 10%. High correlation of cytotoxicity effect was observed between the Cellometer and flow cytometry under all tested conditions.

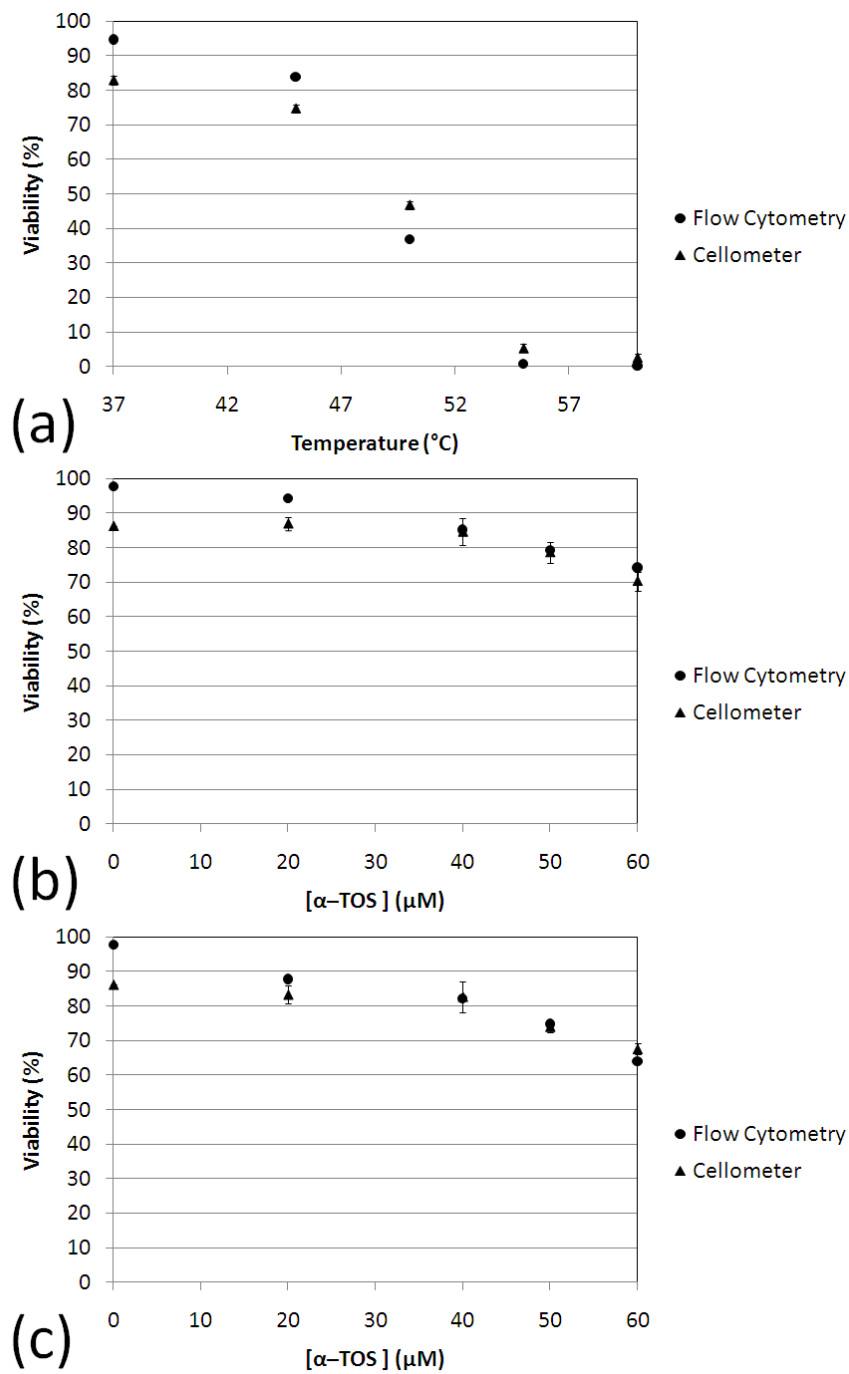


**Figure 4.** Viable cell population percentages were used to plot the viability of Jurkat cells by Cellometer and flow cytometry. The viability dose–response curves for a) heat-induced necrosis, b) drug-induced apoptosis at 24 h, and c) drug-induced apoptosis at 48 h.

**Figure 5. Validation of Cellometer detection**

- (5a) With the Cellometer at 96 h incubation, the dose–response curve of  $\alpha$ -TOS showed an IC<sub>50</sub> at approximately 50  $\mu$ M, where the viability reduced ~40% at 100  $\mu$ M.
- In contrast, QBS induced apoptosis showed a decrease in viability to only 50% at 100  $\mu$ M. The results showed the capability of Cellometer Vision detecting cytotoxicity differences between the two chemical compounds.

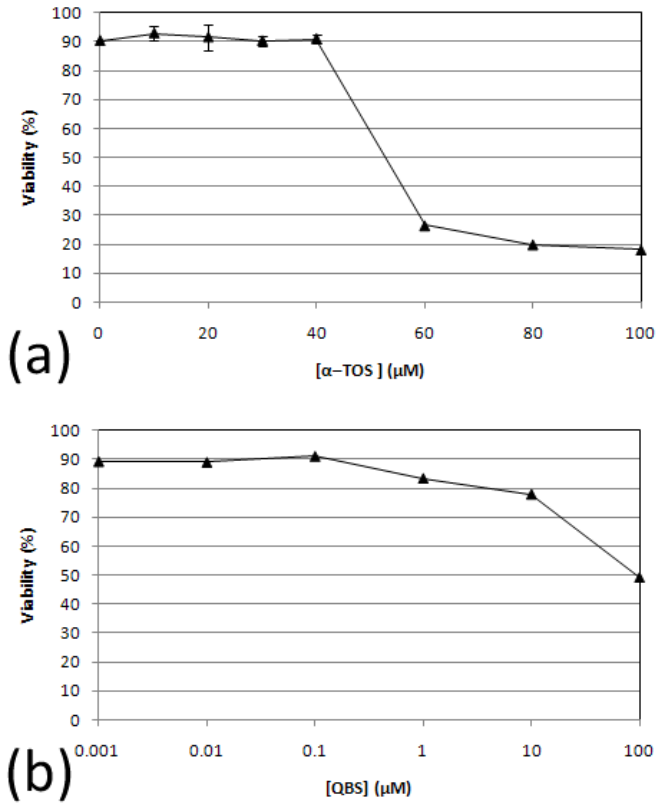


**Figure 5.** Comparison of cytotoxicity dose–response for  $\alpha$ -TOS and QBS by Cellometer. Jurkat cells were incubated with a)  $\alpha$ -TOS and b) QBS.

## Discussion

The ability to perform fluorescence-based necrosis/apoptosis analysis with Cellometer Vision was demonstrated through measuring of heat-induced and drug-induced cell death in Jurkat cells.

### *Heat-induced necrosis*

- The fluorescence intensity scatter plots of Annexin V-FITC with respect to PI showed comparable results ( $\pm 5\%$ ) between Cellometer and flow cytometry, which could be verified with the captured fluorescent images.
- As the temperature increased from 37 to 55°C, Cellometer showed a noticeable increase in the number of apoptotic cells as expected. At 60°C incubation, the physiochemical damage (heat-killed) caused a drastic shift from apoptotic (Annexin V positive only) to necrotic (Annexin V and PI positive) cell populations [8, 9].
- Temperature-dependent viability trends calculated using the fluorescence intensity results from flow cytometry and Cellometer Vision were comparable with a difference of less than 15%. The only significant difference was observed for the 55°C temperature point, where fluorescent images acquired using Cellometer visually indicated that ~45% of cells were PI positive, in contrast to the 90% shown by flow cytometry. Since the flow cytometer and Cellometer Vision counted over 20,000 and 2,000 cells respectively, the differences in number of cells counted between Cellometer and flow cytometry could have contributed to the inconsistency at the 55°C incubation. However, since no visual data was collected from flow cytometry, uncertainties of nonspecific fluorescing debris may have also contributed to the inconsistency. It has also been reported that the shear stress caused by flow during the flow cytometric analysis could be detrimental to cells, which could help explain the lower viability obtained from flow cytometry [10].

### *Chemical-induced apoptosis*

- The fluorescent images visibly showed an increase in the number of apoptotic cells under the FITC fluorescence channel, whereas necrotic cells remained constant. This indicated that the cytotoxic effect of  $\alpha$ -TOS was specific to apoptosis, which was expected with the known effects of  $\alpha$ -TOS [7].
- In the scatter plot, both Cellometer and flow cytometry showed similar increases in apoptotic percentages at 24 and 48 h with respect to  $\alpha$ -TOS concentration. The viability dose-response curve also showed comparable results between Cellometer and flow cytometry with a difference of less than 10%. It seemed that there was only a small decrease in viability when the incubation time was extended to 48 h.
- To further the capability of the imaging-based detection method, the difference in cytotoxicity effect between  $\alpha$ -TOS and QBS was measured using Cellometer. The increase in incubation time (96 h) and concentration of  $\alpha$ -TOS produced a significant

reduction in viability with a noticeable sigmoidal dose–response curve, whereas QBS showed a viability result considerably higher at 100  $\mu\text{M}$ .

- For the drug treatment, Cellometer reported a significant increase in the apoptotic cell population at a much longer incubation time that corresponded to the highly regulated apoptosis process, while minimum change was measured for the necrotic cell population. The results were also highly similar with the known mechanisms of  $\alpha$ -TOS. Taken together, these results validated the capability and reliability of Cellometer as an alternative instrumentation for cell death analysis.

## Conclusion

- The Cellometer imaging cytometry method was able to rapidly obtain fluorescence-based population analysis of necrotic/apoptotic effect induced by heat and chemical compound. The results agreed well with flow cytometry data and were consistent with the known physiochemical damage by heat treatment.
- Using the Cellometer Vision, an apoptosis assay was improved by low sample volume requirement and rapid data acquisition and analysis. In comparison to the 300–500  $\mu\text{L}$  of target sample required for flow cytometry, only 20  $\mu\text{L}$  of sample is required for the Cellometer. Although the number of cells analyzed was dramatically different between the two methods, Cellometer was able to generate consistently comparable results as conventional flow cytometry.
- The ability to record brightfield and fluorescence images allows visualization of cell detection and image analysis, which cannot be done by conventional flow cytometry. Moreover, the lack of high power lasers or photomultiplier tubes in the Cellometer systems eliminates the need for precise optical alignment, so that the system does not require daily user maintenance.
- We have developed and evaluated new applications of Cellometer Vision for fluorescence-based cell death detection assays, which is of great importance to a variety of clinical diagnosis and biomedical research. The ability to rapidly perform cell population analysis including cell morphology, phenotyping, cell concentration and viability measurement at reasonable cost improves research efficiency, especially when a flow or laser scanning cytometer is not available or in situations where a rapid analysis of data is critical.

## References

1. Chan, L.L., et al., Cellometer Vision as an alternative to flow cytometry for cell cycle analysis, mitochondrial potential, and immunophenotyping. *Cytom Part A*, 2011. **79A**(7): p. 507-517.
2. Robey, R.W., et al., Rapid detection of ABC transporter interaction: Potential utility in pharmacology. *J Pharmacol Toxicol Methods*, 2011. **63**: p. 217-222.

3. Chan, L.L., et al., Direct concentration and viability measurement of yeast in corn mash using a novel imaging cytometry method. *J Ind Microbiol Biotechnol*, 2010. **38**(8): p. 1109-1115.
4. Stapelberg, M., et al.,  $\alpha$ -Tocopheryl succinate inhibits proliferation of mesothelioma cells by selective down-regulation of fibroblast growth factor receptors. *Biochemical and Biophysical Research Communications*, 2004. **318**: p. 636-641.
5. Zu, K., L. Hawthron, and C. Ip, Up-regulation of c-Jun-NH<sub>2</sub>-kinase pathway contributes to the induction of mitochondria-mediated apoptosis by  $\alpha$ -tocopheryl succinate in human prostate cancer cells. *Molecular Cancer Therapeutics*, 2005. **4**(1): p. 43-50.
6. Kim, Y.-H., et al., G2 arrest and apoptosis by 2-amino-N-quinoline-8-yl-benzenesulfonamide (QBS), a novel cytotoxic compound. *Biochemical Pharmacology*, 2005. **69**: p. 1333-1341.
7. Neuzil, J., et al., Vitamin E Analogues: A New Class of Inducers of Apoptosis with Selective Anti-Cancer Effects. *Current Cancer Drug Targets*, 2004. **4**: p. 355-372.
8. Yu, M., et al., hMTERF<sub>4</sub> knockdown in HeLa cells results in sub-G<sub>1</sub> cell accumulation and cell death. *Acta Biochimica et Biophysica Sinica*, 2011. **43**(5): p. 372-379.
9. Zhang, P., et al., Identification of genes associated with cisplatin resistance in human oral squamous cell carcinoma cell line. *BMC Cancer*, 2006. **6**: p. 224.
10. Yusof, A., et al., Inkjet-like printing of single-cells. *Lab on a Chip*, 2011. DOI: [10.1039/c1lc20176j](https://doi.org/10.1039/c1lc20176j).